Multiple coupling of surface plasmons in quasiperiodic gratings

Ido Dolev,* Michael Volodarsky, Gil Porat, and Ady Arie

Department of Physical Electronics, Fleischman Faculty of Engineering, Tel-Aviv University, Tel-Aviv 69978, Israel

**Corresponding author: idodolev@tau.ac.il*

Received February 15, 2011; revised March 21, 2011; accepted March 29, 2011;
posted March 30, 2011 (Doc. ID 142733); published April 22, 2011

Whereas periodic gratings enable us to couple light into a surface plasmon polariton only at a specific angle and wavelength, we show here that quasiperiodic gratings enable the coupling of light at multiple wavelengths and angles. The quasiperiodic grating can be designed in a systematic manner using the dual-grid method, thereby enabling us to control the coupling strength and grating dimensions. We verified the method experimentally by efficiently coupling light into a surface plasmon from several different illumination angles using a single quasi-periodic grating.

OCIS codes: 050.2770, 240.6680, 240.5420.

Surface plasmon polaritons (SPPs) are surface electromagnetic waves propagating along the interface of a metal with a negative dielectric constant and a dielectric material with a positive dielectric constant. The SPP plays a key role in many research applications and devices [1], including chemical and biochemical sensors based on enhanced Raman scattering [2], nanoscale metallic waveguides for light [3], and surface-enhanced nonlinear mixers [4]. Coupling of the SPP at the metal–dielectric interface is a challenging task because the wave vector of the SPP is larger than the free-space wave vector. Prisms and periodic gratings are frequently used to allow for efficient coupling of a single free-space wave to a single SPP by matching their wave vectors (momentum). Several techniques have been suggested for more sophisticated plasmon coupling, such as the multidiffraction grating [5], chirped grating [6,7], and coupling in a chiral thin film [8]. In addition, numerical optimization was also suggested to improve coupling with a grating [9]. However, these methods have a limited number of controllable parameters and therefore cannot enable efficient coupling at any arbitrary set of chosen angles and wavelengths. In this Letter, we propose a new method to couple SPPs by using a quasiperiodic grating. This method allows coupling several free-space wave vectors into either a single SPP or several SPPs simultaneously. The quasiperiodic gratings are designed in a systematic manner by adopting a well-known method in the field of quasicrystals—the dual-grid method (DGM) [10,11]. Furthermore, this design method enables us to independently control the coupling strength of each interaction as well as the physical size of the grooves and ridges of the grating coupler (thereby taking into account the manufacturing limitations). Moreover, while here we demonstrate the method with a one-dimensional (1D) grating, the method can be easily extended into the second available dimension of the surface, thus allowing the coupling of light from different directions into the SPPs. The phase-matching conditions for efficient coupling between the free-space wave and the SPP in a periodic grating with period Λ is defined by

$$k_0 \sin\theta + m\frac{2\pi}{\Lambda} = \mp \mathrm{Re}(k_{sp}), \qquad (1)$$

where k_0 and k_{sp} are the free-space and SPP wavenumbers, respectively, θ is the illumination angle relative to the surface normal, and $m = \pm 1, 2, \ldots N$. For semi-infinite metal and dielectric mediums $k_{sp} = k_0 \times [(\varepsilon_m \varepsilon_d)/(\varepsilon_m + \varepsilon_d)]^{0.5}$, where ε_m and ε_d are the permittivities of the metal and the dielectric, respectively. The strength of the coupling of the SPP depends on the value of the Fourier coefficient at the corresponding spatial frequency. It therefore decreases as $|m|$ increases and reaches the maximum value for the first-order coefficient ($m = \pm 1$). Figure 1(a) illustrates such a scheme where the dielectric material is $KTiOPO_4$ (KTP), and the metal is silver. The SPP can be coupled both to the Ag–KTP and to the air–Ag interfaces.

For the coupling of different free-space wave vectors at different illumination angles and into different SPPs, one needs to design a grating that has several well-defined Fourier components. The amplitude of each Fourier component will determine the relative coupling strength. With periodic gratings, one can couple only interactions that are described by Eq. (1) with limited control on the coupling strength. However, a quasiperiodic grating can provide an arbitrary set of Fourier

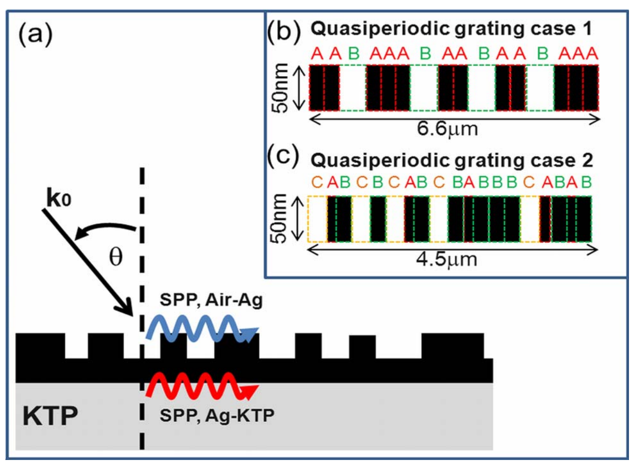

Fig. 1. (Color online) (a) Illustration of the SPP quasiperiodic grating coupler. Inset, part of the quasiperiodic gratings composed of building blocks of lengths (b) A = 386 nm and B = 499 nm and (c) A = 177 nm, B = 229 nm, and C = 314 nm.

0146-9592/11/091584-03$15.00/0

components and is therefore a good candidate for the multicoupling task.

Quasiperiodic structures are structures that exhibit long-range order, which is manifested by a discrete set of well-defined peaks in their Fourier spectra. By using a suitable quasiperiodic grating, we can therefore couple different electromagnetic waves into SPPs simultaneously. For designing such a grating, we have used the DGM [10]. This is a systematic algorithm that enables us to determine the required pattern of the grating so that it will simultaneously couple different interactions with arbitrary wave vector mismatch values. In addition, it also allows us to optimize the amplitudes of the Fourier components for each wave vector mismatch. It is interesting to note that the DGM algorithm was previously used in our group in a nonlinear optical application, for solving the simultaneous phase-matching process of several three-wave mixing interactions [11]. We also note that quasiperiodic plasmonic structures have been studied recently—but for different applications of light transmission through two-dimensional (2D) quasiperiodic nanohole arrays [12–14]. A general model for SPP dispersion relations and mode density on weakly corrugated quasiperiodic surface has been suggested [15], and a detailed analysis for two specific quasiperiodic gratings (Fibonacci and Thue-Morse) [16] has been performed. However, in these structures [15,16], the parameters of the Fourier spectra are already defined and cannot be tailored to couple SPPs at arbitrary frequencies; hence, they do not provide the full design flexibility of coupling to SPPs that we show here.

To demonstrate the DGM SPP coupling, we designed five different structures: three periodic gratings with a duty cycle of 0.5 and periods of $\Lambda_1 = 1.03\,\mu$m, $\Lambda_2 = 0.79\,\mu$m, and $\Lambda_3 = 0.58\,\mu$m and two quasiperiodic gratings.

The periodic gratings Λ_1, Λ_2, and Λ_3, were designed to support air–Ag (Ag-KTP) SPP, which are generated by illumination with $\lambda = 1047.5$ nm with incidence angles of 1° (62°), 17° (36°), and 51° (6°), respectively. The quasiperiodic gratings were generated with the DGM, which produces the quasiperiodic order in which a set of real space tiles is placed. For the first quasiperiodic grating, the design goal was to support the two different $\Delta k's$:$\Delta k_1 = 2\pi/\Lambda_1$ and $\Delta k_2 = 2\pi/\Lambda_2$ (case 1). The corresponding tiling lengths are 0.386 and 0.499 μm [11]. The Fourier coefficient's amplitude of each supported wave vector mismatch can be controlled by determining the duty cycle of each tile, i.e., the relative part of it that constitutes a groove [17]. By numerically scanning over the possible values of the duty cycles in each one of the building blocks, we have found that a nearly equal and maximum Fourier coefficient of ~0.4 for both wave vector mismatches is achieved with duty cycles of 1 (i.e., building block A is a ridge) and 0 (B is a groove) as illustrated in Fig. 1(b). For comparison, the amplitudes of the Fourier coefficients are $2/\pi \sim 0.63$ for the periodic gratings. The second quasiperiodic grating was designed to support all three Δk's: Δk_1, Δk_2, and $\Delta k_3 = 2\pi/\Lambda_3$ (case 2). This time we chose to numerically optimize Δk_3; hence, its Fourier coefficient amplitude is equal to 0.4 and is much bigger than the amplitudes of the Fourier coefficient of Δk_1 (0.18) and Δk_2 (0.27), as shown in Fig. 2. In this case, the tiling lengths were 0.177, 0.229,, and 0.314 μm with duty cycles of 1, 1, and 0, respectively, as illustrated in Fig. 1(c).

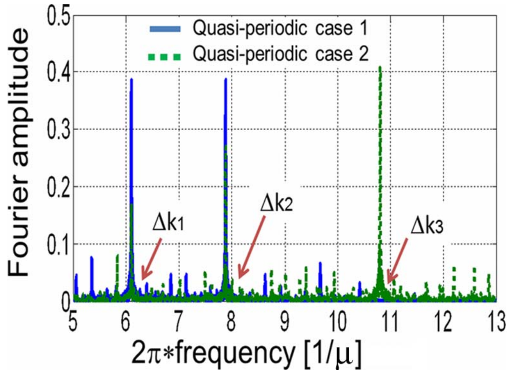

Fig. 2. (Color online) Fourier spectra of the quasiperiodic gratings used for SPP coupling experiments.

The samples were prepared by evaporating 25 nm of silver film on top of a KTP crystal followed by a standard *e*-beam lithography technique to generate the desired structure on a PMMA (polymethyl methacrylate) mask. A 50 nm silver layer was then evaporated, and the PMMA was removed. The result was a 50 nm silver grating and a 25 nm silver film on top of the KTP dielectric crystal (Fig. 1). The size of each grating was 400 μm × 400 μm.

We verified that the gratings support the desired wave vector mismatches by performing diffraction experiments (wavelength 532 nm). As expected, we observe the first diffraction order at angles of 31° and 42° for the periodic gratings [Figs. 3(a) and 3(b)], and two diffraction orders at the same angles for the quasiperiodic (case 1) structure [Fig. 3(c)]. This indicates that the quasiperiodic grating has both Δk_1 and Δk_2 components in its Fourier spectrum.

We performed a reflection experiment in order to characterize the coupling into the SPP, which will be manifested as a reflection dip at the coupling angle: a 200 mW, Nd:YLF CW laser (1047.5 nm) was focused to a waist of 200 μm. The laser polarization was set by a half-wave plate and a polarizer to TM polarization. The gratings were set on a rotating stage, and the reflected light was measured at 0.5° steps. The results are presented in Fig. 4. The reflection versus illumination angles were also simulated at 0.1° steps, for $\varepsilon_{\text{silver}} = -56.09 + 0.59i$ and

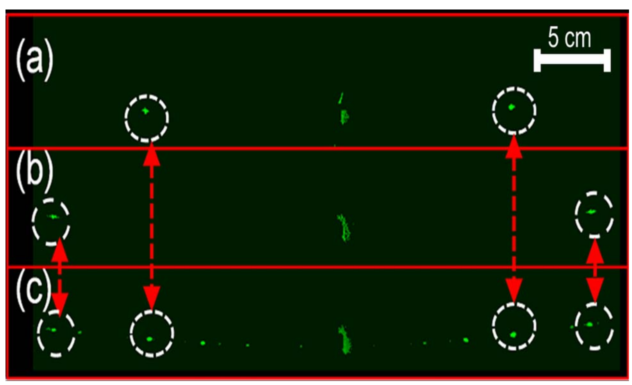

Fig. 3. (Color online) Light diffraction at a distance of 20 cm from the samples for the periodic grating (a) Λ_1, (b) Λ_2, and (c) dual-frequency quasiperiodic grating.

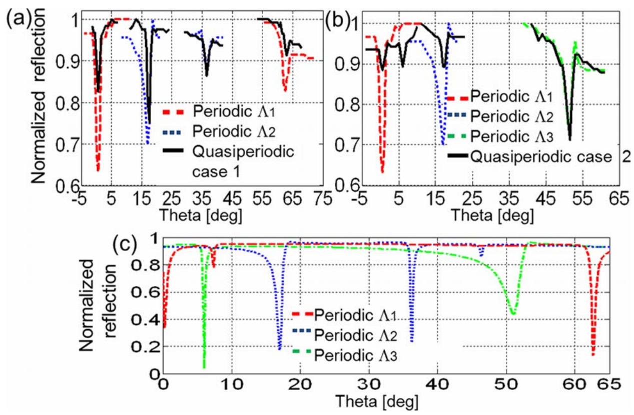

Fig. 4. (Color online) Normalized reflection versus illumination angle for the different gratings: (a), (b) experimental results and (c) simulation results.

$\varepsilon_{\mathrm{KTP}} = 3.35$, with rigorous coupled-wave analysis (RCWA). As shown in Fig. 4(c), the angles of the reflection dips of the periodic gratings were almost identical to the simulation (with deviation of $<0.5°$). Nevertheless, the efficiencies of the coupling were lower than in the simulation, especially for the Ag–KTP plasmons. This deviation from theory is mostly due to imperfection in the manufacturing process (the film and the grating thicknesses and quality as well as the KTP surface roughness).

In Fig. 4(a) we present the measurements of the periodic gratings (Λ_1 and Λ_2) air–Ag and Ag–KTP SPP and the case 1 quasiperiodic grating. As predicted, all SPPs are coupled in the quasiperiodic grating at the exact angles as the SPP from the periodic gratings. This implies that a single quasiperiodic grating can be used to couple several SPPs simultaneously.

Figure 4(b) presents similar measurements of the air–Ag SPP for all three periodic gratings and for the case 2 quasiperiodic grating. Again, all air–Ag SPPs appear in the single quasiperiodic grating at identical angles as the SPP in the periodic gratings. An additional dip appears in the case 2 quasiperiodic grating corresponding to the Ag–KTP SPP (Δk_3 mismatch). The Ag–KTP SPPs corresponding to Δk_1 and Δk_2 mismatches in the case 2 quasiperiodic grating were not detected due to their relatively low Fourier amplitudes and the imperfection in the manufacturing process. The coupling of the SPP with a quasiperiodic grating indicates that the long-range order, well-defined grating momentum, plays an important role in the SPP coupling mechanism.

As predicted by its Fourier coefficient amplitudes, the coupling strengths of the measured quasiperiodic SPP are lower than that of the periodic gratings. Nevertheless, they can be tuned and engineered by choosing the proper Fourier coefficient amplitudes. This is demonstrated experimentally in the case 2 quasiperiodic grating: the Fourier coefficient amplitude that fits to Δk_3 mismatch was maximized (Fig. 2), producing strong coupling to the corresponding SPP [Fig. 4(b)].

In the above experiments, we coupled the same wavelength from several different angles to a single SPP. This method can also be used for the coupling of different wavelengths in the same or different angles to the same or different SPPs. The DGM algorithm inputs are the Δk's mismatch values; hence, by solving Eq. (1) for each case (wavelength, angle, and k_{sp}) and using the Δk's as the DGM inputs—coupling of several wavelengths/angles/SPPs is possible. This could be useful for nonlinear mixing applications of the SPPs, which require coupling of several wavelengths simultaneously [3,18]. Moreover, this method is not limited to the 1D grating; 2D quasiperiodic structures can also be realized with DGM [11], which can be then used for multiple SPP 2D couplers.

In summary, we have shown a method of coupling a SPP using a quasiperiodic grating. This robust method allows control and optimization on the coupling strength. Our experiments indicate the importance of a long-range order (momentum) for SPP grating coupling. We demonstrated experimental coupling of the SPP from several different illumination angles using one quasiperiodic grating. This SPP coupling technique can be used for a wide range of applications where multiple coupling conditions are required, such as biochemical SPP sensors, nonlinear optics, and other SPP subwavelength optical devices.

We thank H. Feldman for providing the RCWA simulation code and A. Tsukernik for the *e*-beam writing. This work was supported by the Israel Science Foundation through grant 774/09.

References

1. S. A. Maier, *Plasmonics: Fundamentals and Applications* (Springer, 2007).
2. J. Homola, S. S. Yee, and G. Gauglitz, Sens. Actuators B **54**, 3 (1999).
3. W. L. Barnes, A. Dereux, and T. W. Ebbesen, Nature **424**, 824 (2003).
4. S. Palomba and L. Novotny, Phys. Rev. Lett. **101**, 056802 (2008).
5. P. Adam, J. Dostalek, and J. Homola, Sens. Actuators B **113**, 774 (2006).
6. M. Martl, J. Darmo, K. Unterrainer, and E. Gornik, in *Conference on Lasers and Electro Optics* (Optical Society of America, 2008), paper JWA43.
7. W. Yeh, J. Kleingartner, and A. C. Hillier, Lett. Anal. Chem. **82**, 4988 (2010).
8. Devender, D. P. Pulsifer, and A. Lakhtakia, Electron. Lett. **45**, 1137 (2009).
9. G. Leveque and J. F. Martin, J. Appl. Phys. **100**, 124301 (2006).
10. N. G. de Bruijn, Proc. K. Ned. Akad. Wet., Ser. A: Math. Sci. **84**, 39 (1981).
11. R. Lifshitz, A. Arie, and A. Bahabad, Phys. Rev. Lett. **95**, 133901 (2005).
12. D. Pacifici, H. J. Lezec, L. A. Sweatlock, R. J. Walters, and H. A. Atwater, Opt. Express **16**, 9222 (2008).
13. F. Przybilla, C. Genet, and T. W. Ebbesen, Appl. Phys. Lett. **89**, 121115 (2006).
14. T. Matsui, A. Agrawal, A. Nahata, and Z. V. Vardeny, Nature **446**, 517 (2007).
15. J. M. Pereira, Jr., E. L. Albuquerque, G. A. Farias, and R. N. Costa Filho, Phys. Rev. B **72**, 045433 (2005).
16. J. M. Pereira, Jr., G. A. Farias, and R. N. Costa Filho, Eur. Phys. J. B **36**, 137 (2003).
17. A. Bahabad, N. Voloch, A. Arie, and R. Lifshitz, J. Opt. Soc. Am. B **24**, 1916 (2007).
18. M. Volodarsky, I. Dolev, Y. Sivan, T. Ellenbogen, and A. Arie, in *Frontier in Optics Conference* (Optical Society of America, 2010), paper FThB8.